Glass behaviour in the solid solution of deuterated betaine phosphate$_{0.15}$ betaine phosphite$_{0.85}$

2000 J. Phys.: Condens. Matter 12 201

(http://iopscience.iop.org/0953-8984/12/3/301)

J. Phys.: Condens. Matter **12** (2000) 201–211. Printed in the UK PII: S0953-8984(00)06751-5

Glass behaviour in the solid solution of deuterated betaine phosphate$_{0.15}$ betaine phosphite$_{0.85}$

J Banys†‖, C Klimm†, G Völkel†, H Schäfer†, A Kajokas‡ and A Klöpperpieper§

† Fakultät für Physik, Universität Leipzig, D-04103 Leipzig, Germany
‡ Faculty of Physics, Vilnius University, 2040 Vilnius, Lithuania
§ Fachbereich Physik, Universität des Saarlandes, D-66123 Saarbrücken, Germany

Received 9 August 1999, in final form 12 November 1999

Abstract. For a deuterated solid solution of 15% antiferroelectric betaine phosphate (BP) and 85% ferroelectric betaine phosphite (BPI), measurements of the dielectric permittivity at frequencies 20 Hz $< \nu <$ 1 MHz are reported. The freezing phenomena in $DBP_{0.15}DBPI_{0.85}$ reveal the characteristics of a transition into a dipolar glass state with peculiarities due to the quasi-one-dimensional structure. Using the Kutnjak model a glass temperature of 25 K is estimated for deuterated $DBP_{0.15}DBPI_{0.85}$ and one of 10 K for protonated $BP_{0.15}DBPI_{0.85}$. The relaxation time distribution extracted from the experimental data by means of Tikhonov regularization and calculated in the region of the dielectric dispersion shows an asymmetric behaviour especially at lower temperatures, which is interpreted as being caused by a Gaussian distribution of activation energy and double-well potential asymmetry as well.

1. Introduction

The compounds betaine phosphate (BP: $(CH_3)NCH_2COOH_3PO_4$) and betaine phosphite (BPI: $(CH_3)NCH_2COOH_3PO_3$) are molecular crystals of the amino acid betaine and phosphoric and phosphorous acid, respectively. In both compounds the inorganic components (PO_4 or PO_3 groups) are linked by hydrogen bonds to quasi-one-dimensional chains [1]. BP exhibits a ferroelastic phase transition at about 365 K followed by two phase transitions at 86 K and 81 K [1]. Antiferroelectric order is established at $T_C = 86$ K [2]. At this temperature the O–H$\cdots$O bonds order along the one-dimensional chains and the chains are linked antiferroelectrically [3]. At 355 K BPI transforms into an elastically ordered state and exhibits ferroelectric order below $T_C = 216$ K [1, 4]. The two almost isostructural compounds form solid solutions at any concentration [4]. It has been shown that at intermediate concentrations the long-range electric order is suppressed [4] and no spontaneous polarization occurs [5, 6]. The mixed crystal $BP_{0.4}BPI_{0.6}$ exhibits relaxational behaviour typical for an orientational glass state [7], with a hindering barrier $E_b/k_b = 252$ K. Investigations of the dielectric properties of $BP_{0.15}BPI_{0.85}$ showed freezing phenomena typical for the transition into a dipolar glass state. The activation energy was found to be $E_b/k_b = 518$ K [9].

Deuteration of hydrogen-bonded ferroelectrics leads to significant changes of the dielectric properties and shifts the phase transition temperature to higher values [10]. This isotope effect has already been studied in deuterated crystals of the betaine family, namely betaine

‖ On leave from: Faculty of Physics, Vilnius University, Lithuania.

0953-8984/00/030201+11$30.00

phosphate (DBP) and betaine phosphite (DBPI) [2, 11]. The low-frequency dielectric measurements of DBPI showed [11] that the transition temperature is shifted up to 297 K. Dielectric investigations of γ-irradiated $DBP_{0.15}DBPI_{0.85}$ showed a lower activation energy $E_b/k_b = 311.6$ K and a higher estimated glass temperature [12] $T_G = 55.4$ K as compared with the non-deuterated sample of $BP_{0.15}BPI_{0.85}$. The local proton and deuteron order in $BP_{0.15}BPI_{0.85}$ and $DBP_{0.15}DBPI_{0.85}$ has been recently investigated using high-resolution electron paramagnetic resonance (EPR) spectroscopy techniques such as electron–nuclear double resonance (ENDOR) and electron spin-echo envelope modulation (ESEEM) [13, 14]. The results showed that the random-bond random-field (RBRF) Ising model explains quite well the temperature behaviour of $DBP_{0.15}DBPI_{0.85}$, whereas proton tunnelling has to be taken into account for the explanation of the experimental results for $BP_{0.15}BPI_{0.85}$. Surprisingly, it has also been demonstrated that a kind of local proton order still exists within the chains below 150 K in these mixed crystals [14], which can be understood as an intra-chain order as will be shown in the present paper.

In this paper the results of dielectric investigation of deuterated betaine $phosphate_{0.15}$ betaine $phosphite_{0.85}$ in the region of the low-frequency dielectric dispersion are presented. The distribution of relaxation times is extracted from the complex dielectric spectra by using the Tikhonov regularization technique [15] and simulated assuming a distribution of both the activation energy and the attempt frequency. On the other hand, the analysis and comparison of the dielectric data for the deuterated and protonated samples is done according to the Kutnjak model [16] leading to a more accurate glass temperature.

2. Experimental procedure

$DBP_{0.15}DBPI_{0.85}$ crystals were grown by controlled evaporation from D_2O solution containing betaine with 85% of H_3PO_3 and 15% H_3PO_4. By analogy with DBPI [11] one expects that only the protons in the O–H$\cdots$O bonds of the inorganic H_3PO_3 and H_3PO_4 groups should be replaced by deuterons. For the dielectric spectroscopy, gold-plated single crystals were oriented along the monoclinic b-axis. The complex dielectric constant $\varepsilon^* = \varepsilon' - i\varepsilon''$ was measured by a capacitance bridge HP4284A in the frequency range 20 Hz to 1 MHz. The typical sample size was 50 mm^2 area and 1 mm thickness. The value of the measurement voltage was 0.5 V. Further decrease of the measurement voltage does not change the results for the dielectric permittivity. All measurements have been performed on heating with the rate of about 0.1 K min^{-1} in the dielectric dispersion region. No differences in the value of the dielectric permittivity have been observed for cooling and heating due to the low value of the measurement field and the absence of temperature gradients in the sample. The temperature was measured with a calibrated silicon diode (Lake Shore type DT-470-DI-13). For the temperature-dependent measurements a Leybold VSK-4-320 cryostat was used.

3. Results and discussion

For $DBP_{0.15}DBPI_{0.85}$ no anomaly in ε' indicating a polar phase transition can be detected down to the lowest temperatures. A Curie–Weiss law is valid for ε' in the temperature range between 300 K and 200 K with Curie–Weiss constant $C_{CW} = 29\,238$ K, and $T_C = 83$ K (see the inset in figure 1(a)). A much better fit can be achieved using a quasi-one-dimensional Ising model. In this case the static dielectric constant can be expressed [17] by

$$\varepsilon' = C/\left\{T(\exp(-2J_\parallel/k_BT) - J_\perp/k_BT)\right\} \tag{1}$$

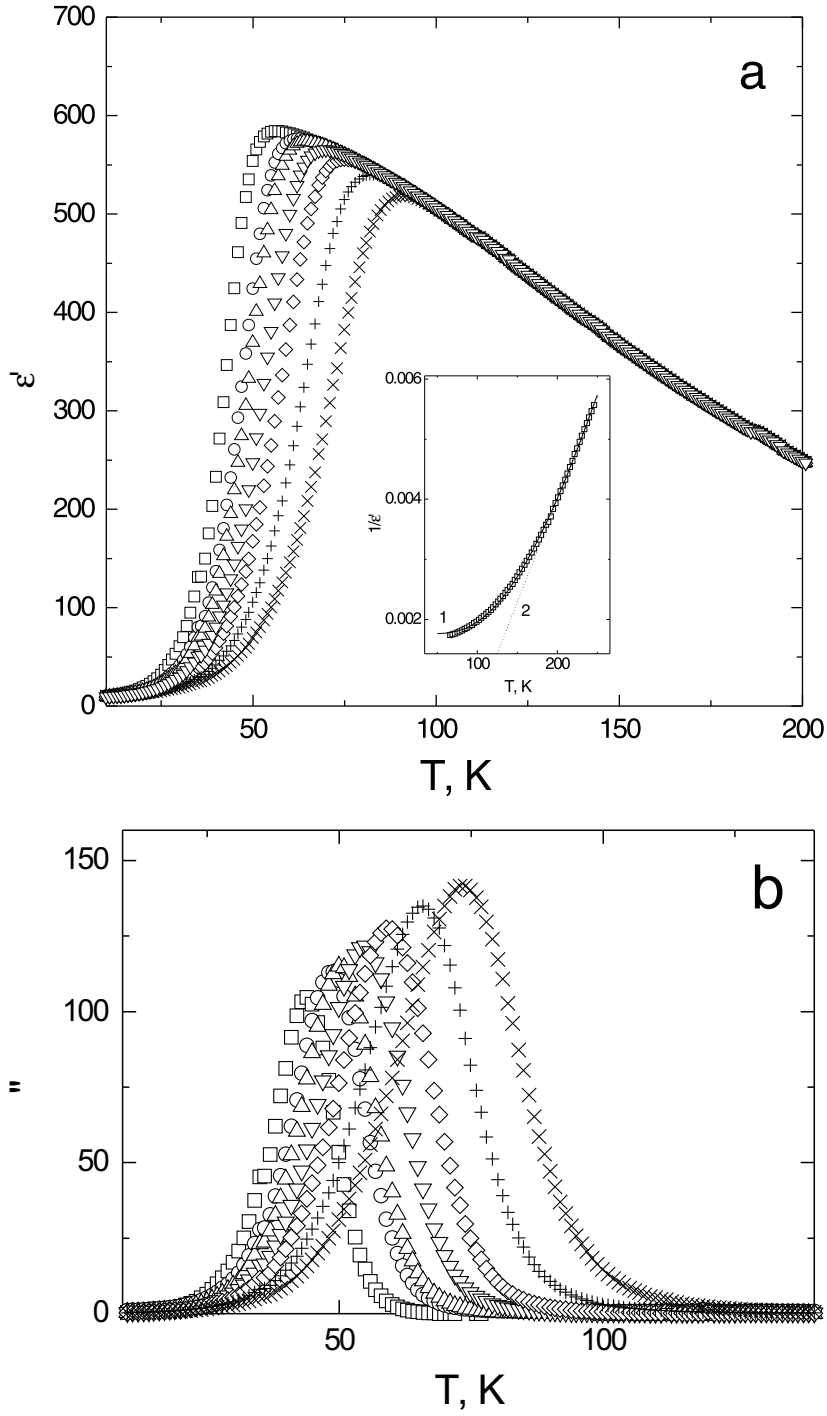

Figure 1. Temperature dependences of ε' (a) and ε'' (b) for $DBP_{0.15}DBPI_{0.85}$ at the following frequencies (kHz): □: 0.1; ○: 1; △: 2; ×: 10; ▽: 40; ◇: 200; +: 1000. The inset shows the temperature dependence of $1/\varepsilon'$ for $DBP_{0.15}DBPI_{0.85}$ at the frequency 100 Hz. Dashed line: the fit with the Curie–Weiss law; solid line: the fit with the quasi-one-dimensional Ising model.

where $J_\parallel$ and $J_\perp$ are the nearest-neighbour intra-chain and the effective mean-field inter-chain coupling constants, respectively, and k_B is the Boltzmann factor. From the best fit in the temperature range between 300 K and 70 K we have obtained the values $C = 15\,820$ K, $J_\parallel/k_b = 172.5$ K, and $J_\perp/k_b = -27.9$ K. The negative sign of $J_\perp$ means that 15% of the antiferroelectric phosphate units are able to change the inter-chain interaction coupling from a ferroelectric one in ferroelectric phosphite to an antiferroelectric one in the mixture due to a decrease of the correlation distance between dipoles.

In the temperature region between 100 K and 20 K dispersion effects dominate the dielectric response in the frequency range under study (figures 1(a) and 1(b)). The temperature–frequency behaviour of ε' and ε'' is typical glassy behaviour: with decreasing measurement frequency the maximum of ε' shifts to lower temperatures followed by the maximum of ε''. It is interesting to note that the absolute value of ε' is nearly three times higher than for the non-deuterated sample $BP_{0.15}BPI_{0.85}$ [9]. The frequency dependence of ε' and ε'' at fixed temperatures provides clear evidence that the frequency dependence of ε'' is much broader than that over 1.14 decades typical for the Debye dispersion (figure 2). The freezing phenomena in $DBP_{0.15}DBPI_{0.85}$ reveal the characteristics of a transition into a dipolar glass state. The slowing down of the dipolar degrees of freedom exhibits a broad distribution of relaxation times, as has been studied in detail for the most prominent dipolar glasses such as $K_{1-x}Li_xTaO_3$ [18], $Rb_{1-x}(NH_4)_xH_2PO_4$ [19], $Rb_{1-x}(NH_4)_xH_2AsO_4$ [20, 21], with a distribution width exceeding by orders of magnitude the width of a monodispersive Debye process [22, 23]. In orientational glasses (OG) the reorienting moments freeze in random configurations [24]. The interplay of site disorder and frustrated interactions is responsible for the freezing transition which bears similarities with the spin-glass transitions in dilute magnetic systems [25] and with the relaxational dynamics in canonical glasses [24].

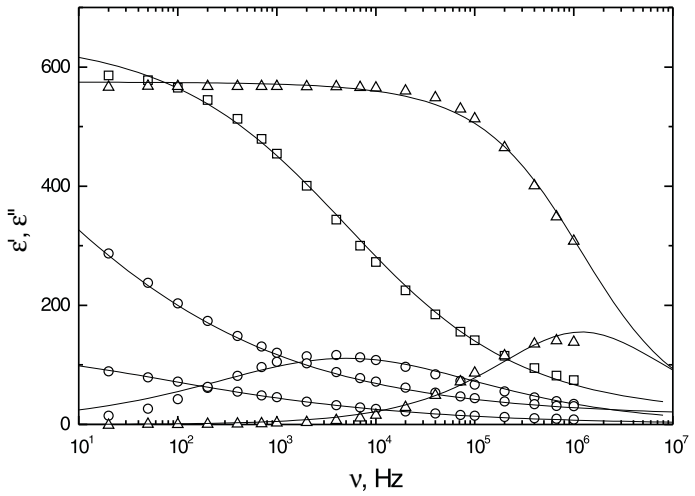

Figure 2. The frequency dependences of ε' and ε'' for $DBP_{0.15}DBPI_{0.85}$ at the temperatures (K): △: 71; □: 51; ○: 39.

First, the experimental data are fitted to the Cole–Cole function [26]:

$$\varepsilon^* = \varepsilon_\infty + \Delta\varepsilon/(1 + (\mathrm{i}\omega\tau)^{1-\alpha}) \tag{2}$$

where $\Delta\varepsilon$ is the relaxator strength, τ is the most probable relaxation time, α is the distribution coefficient, ε_∞ is the contribution of all higher-frequency modes to the dielectric permittivity, and $\omega = 2\pi\nu$ is the angular velocity. The data calculated using the Cole–Cole formula are shown as solid lines in figure 2. The temperature dependences of the fit parameters $\Delta\varepsilon$, α, and τ are shown in figure 3. The distribution function of the relaxation time τ for the Cole–Cole

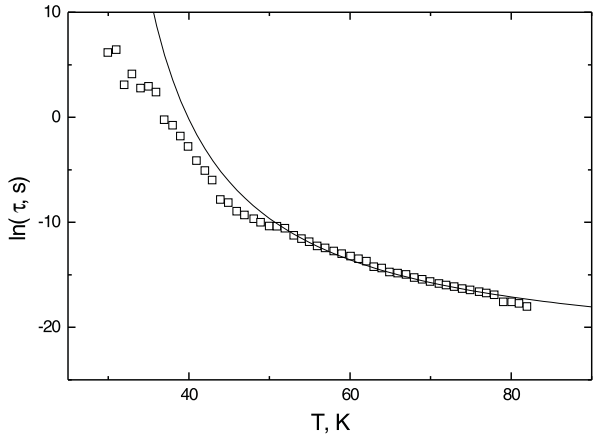

(a)

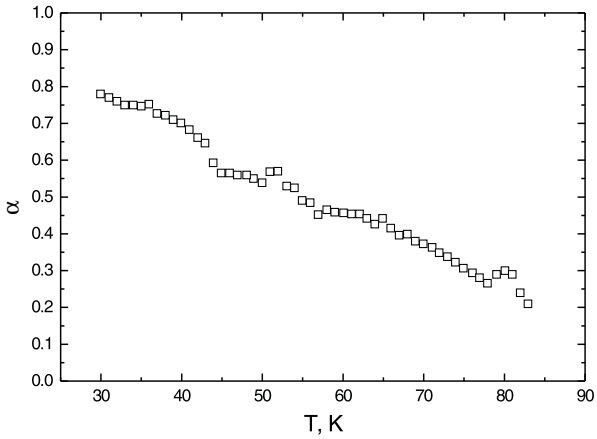

(b)

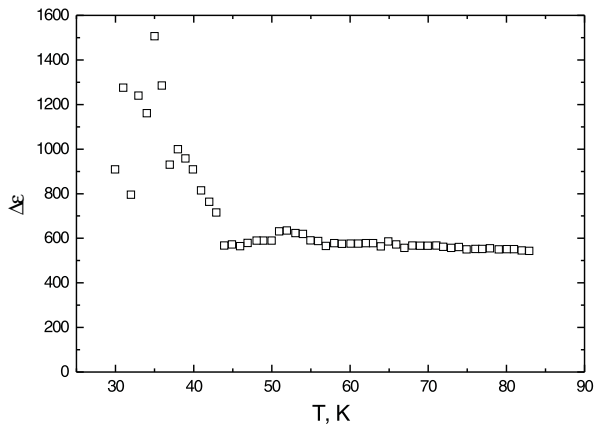

(c)

Figure 3. Temperature dependences of the fit parameters τ (a), α (b) and $\Delta\varepsilon$ (c) for $DBP_{0.15}DBPI_{0.85}$. The parameters of the line drawn according to a Vogel–Fulcher law in (a) are given in the text.

function is symmetrically shaped around the most probable relaxation time. When $\alpha > 0.5$ the relaxation times are distributed over three decades. Such a wide distribution of relaxation times can mean that non-equilibrium effects or quantum fluctuations play a significant role at those temperatures where α reaches high values. The most probable relaxation time follows a Vogel–Fulcher law $\tau = \tau_0 \exp\{E_b/k_b(T - T_0)\}$, with $\tau_0 = 9 \times 10^{-11}$ s, $E_b/k_b = 330$ K, and $T_0 = 26$ K as indicated by the solid line in figure 3(a). The activation energy E_b/k_b is bigger than that at 252 K in $BP_{0.4}BPI_{0.6}$ [7] and close to that at 290 K in pure deuterated betaine phosphite [8] but nearly twice lower than in pure BPI as measured by ^{1}H ENDOR [27] and dielectric measurements [28]. The deviation of the fit from the experimental points at the low-temperature end of the temperature scale of figure 3(a) is caused by the shortcomings of the Cole–Cole model as shown in the next section. Below the transition temperature into the glassy state the protons are frozen in at random in their double-minima potentials, as in RADP [19], but along the one-dimensional chains.

A careful inspection of figure 2 shows that the imaginary part of the dielectric permittivity is not exactly symmetrically shaped as it should be in the case of a real Cole–Cole dispersion. Such an asymmetry has already been observed in $BP_{0.6}BPI_{0.4}$ [7]. Instead of using other models like the Havriliak–Negami or Kohlrausch–Williams–Watts ones, we extracted the exact distribution function $f(\tau)$ of the relaxation times τ from the complex dielectric data represented by the general equation

$$\varepsilon^* = \varepsilon_\infty + \int_0^{+\infty} \frac{f(\tau)}{1 + \mathrm{i}\omega\tau}\,\mathrm{d}\tau. \tag{3}$$

The algorithm used is based on solving this integral equation of Fredholm type using the Tikhonov regularization technique with a self-consistent choice of the regularization parameters. The method has been explained in detail in reference [15]. Another paper applying this technique to deuterated rubidium ammonium dihydrogen phosphate appeared recently [30]. The values of ε^* were taken from the experiment. The distribution functions obtained at different temperatures are presented in figure 4. Whereas at higher temperatures

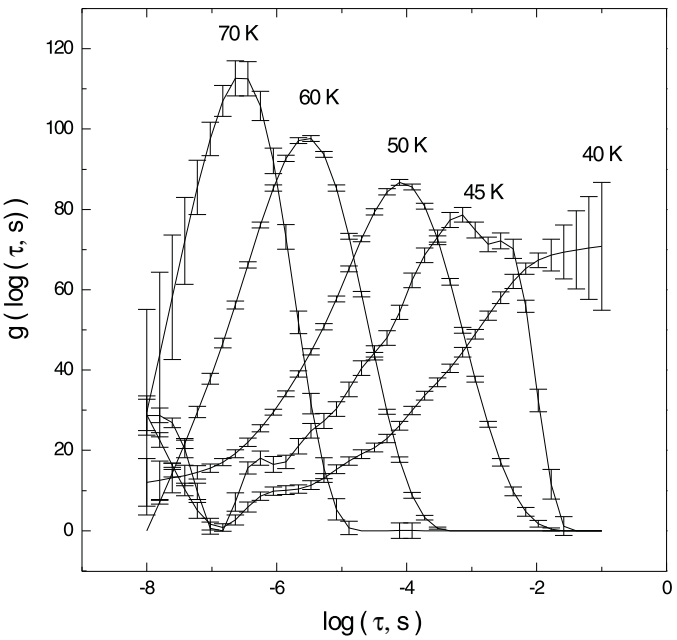

Figure 4. Relaxation time distributions at different temperatures obtained by Tikhonov regularization from equation (3). The error bars show the range of confidence provided by the algorithm.

the relaxation time distribution function appears to be symmetrical and can be described well by a Cole–Cole-type distribution, it becomes asymmetrical with decreasing temperature, and the relaxation time distribution width increases considerably. At lower temperatures the dielectric relaxation times are very asymmetrically distributed with a long tail towards to shorter relaxation times or higher frequencies. Due to this, the mean relaxation time of the distribution and the most probable relaxation time no longer agree one with another. Consequently, as the application of the Cole–Cole model is no longer allowed for the data analysis, it leads to the wrong τ-values at lower temperature as seen in figure 3(a).

The temperature-dependent width and asymmetry of the relaxation time distribution can easily be simulated (see figure 5) by assuming a distribution of the activation energy E_b and the inverse attempt frequency τ_0 as well. As shown in reference [31], the correlation time for uncorrelated hopping over the barrier in an asymmetric double-minimum potential obeys the form

$$\tau = \tau_\infty \frac{\exp\{E_b/k_B(T - T_0)\}}{2\cosh(A/2k_BT)} \tag{4}$$

where the activation energy E_b is a measure of the potential step size and A is the asymmetry of the double-well potential related to the local site polarization. Taking into account the Gaussian distributions of both parameters around their mean values $E_{b_0}/k_B = 330$ K and $A_0/k_B = 0$ K with variances $\sigma_E/k_B = 40$ K and $\sigma_A/k_B = 400$ K, respectively, the numerical simulation fits the experimental relaxation time distribution shown in figure 4 rather well. The numerical simulation with 12 000 items, $\tau_\infty = 10^{-9}$ s, and $T_0 = 25$ K is presented in figure 5 for the same temperatures as in figure 4.

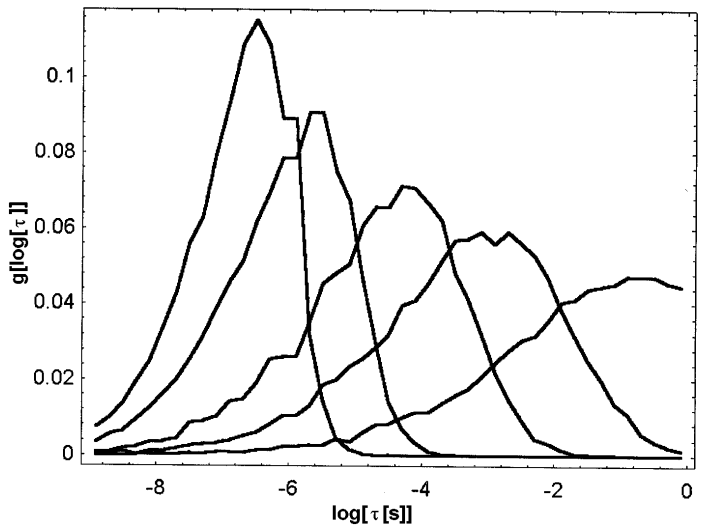

Figure 5. Simulation of the relaxation time distributions at the same temperatures as in figure 4 by means of equation (4) with the parameters given in the text.

This result is in fact a little surprising as regards the zero mean of the asymmetry of the double-well potentials, inasmuch as the ENDOR results for non-deuterated $BP_{0.15}BPI_{0.85}$ [13,14] clearly showed a non-zero mean of the local proton polarizations of the hydrogen bonds in the chain coinciding with a non-zero mean of their local potential asymmetry. As regards

the dielectric data, however, only a zero average of the asymmetry $A_0 = 0$ corresponding to a zero average of the electric polarization leads to a successful simulation. It appears to be very implausible that this discrepancy arises due to deuteration. In fact, the dielectric relaxation is concerned with the reorientation of elementary electric dipolar moments and not with that of single hydrogen bonds. The elementary electric dipolar moments could be clusters of hydrogen bonds within a chain or even a single chain itself. The relatively low attempt frequency $1/\tau_\infty = 10^9$ s^{-1} indicates a large mass of the elementary dipoles and supports this explanation. As mentioned above, the temperature dependence of ε' showed that the inter-chain interaction is antiferroelectric in the mixture. The experimental results mean then that the average local proton polarization measured by the local magnetic resonance technique is not tantamount to a long-range global ferroelectric or antiferroelectric order but expresses the local order within a single chain or in a part of it. From the comparison with the ENDOR results one can conclude that betaine phosphate/phosphite mixed crystals behave like a proton glass without any long-range order. However, the presence of the one-dimensional structure of the phosphate/phosphite chains linked by hydrogen bonds has an interesting consequence. Because of the much stronger intra-chain coupling of the protons with respect to that to neighbouring chains, $|J_\parallel/J_\perp| \simeq 6.2$, a local proton order within a chain is developed independently of that in neighbouring chains below a temperature of about 150 K that has not yet been observed in other proton glasses.

Because of the asymmetric distribution of relaxation times, the observed experimental data were additionally analysed using the model suggested by Kutnjak *et al* [16]. The idea of this model is to get rid of any shape of the distribution function of the relaxation times. For this purpose, the variable $\delta(\nu) = [\varepsilon'(\nu) - \varepsilon_\infty]/[\varepsilon_S - \varepsilon_\infty]$ is introduced with ε_S and ε_∞ denoting static and high-frequency permittivities. By determining the value of the frequency ν_δ for a given δ and for all accessible temperatures, it is possible to construct an Arrhenius plot, the so-called δ-plot, shown in figure 6(a). Notable cases are $\delta \to 0$ and $\delta \to 1$ which correspond to the high- and low-frequency ends of the spectrum of relaxation times. Most interesting is, of course, the limit $\delta \to 1$, which reveals the temperature evolution of the slowest element in the spectrum and which is most important for slow motion or glass freezing.

From figure 6(a) it is evident that for $\delta > 0.9$ the deviation from the Arrhenius behaviour is manifested as a bend of the Arrhenius plot. The solid lines in this figure have been calculated using the Vogel–Fulcher expression with a δ-dependent Vogel–Fulcher temperature. Due to the rather low value of T_0 it is not possible to observe a significant bend of the δ-curves even at low values of δ. In figure 6(b) we show T_0 as a function of δ for $0.9 < \delta < 0.95$. It is clearly seen that for $\delta \to 1$ the Vogel–Fulcher temperature extrapolates to 24.8 K. This value is in good agreement with the value obtained from the temperature behaviour of the most probable relaxation time.

The same model has been used for the non-deuterated sample $BP_{0.15}BPI_{0.85}$. The results are shown in figures 7(a) and 7(b) with an extrapolated Vogel–Fulcher temperature $T_0 = 10$ K.

4. Conclusions

Finally, one can conclude that protonated and deuterated $BP_{0.15}BPI_{0.85}$ exhibit an orientational glass state at low temperatures where the protons or deuterons are frozen in along the one-dimensional chains. The value of the activation energy $E_a/k_B = 330$ K clearly manifests that the orientational order is related to the proton or deuteron order, showing typical activation energies ranging from 200 K to 900 K [29,31]. In contrast to the case for other proton glasses, as a result of the quasi-one-dimensional structure of the phosphate/phosphite chains formed by the hydrogen bonds, a local intra-chain order of the protons sets in far above the glass transition

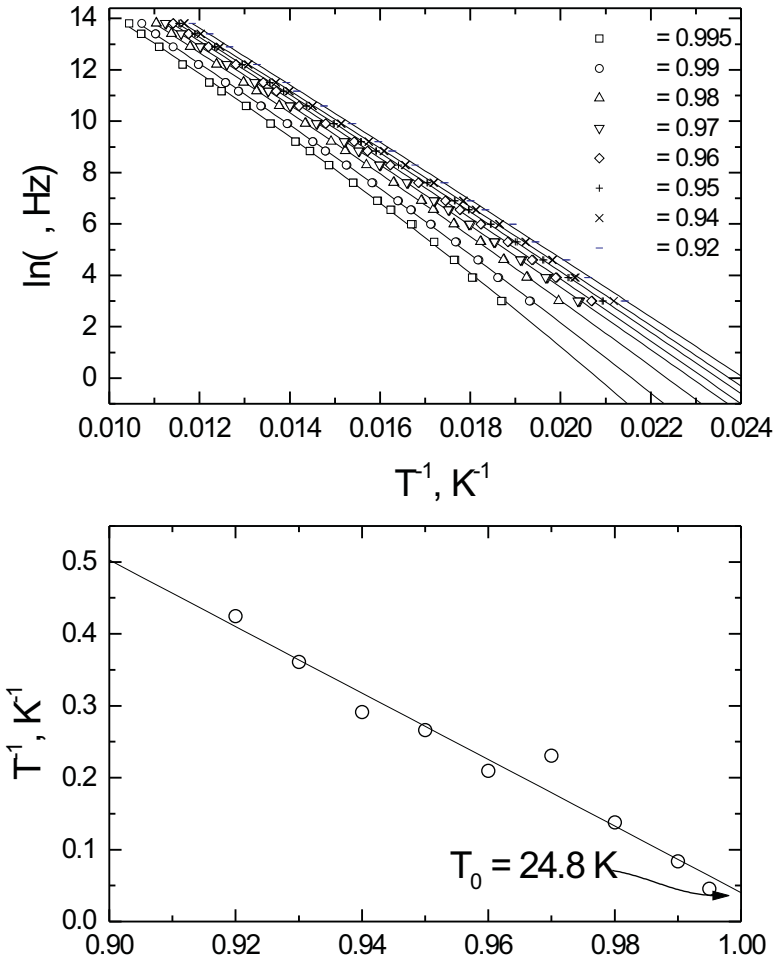

Figure 6. The Arrhenius representation (δ-plot) of $DBP_{0.15}DBPI_{0.85}$ where the points are obtained from the reduced dielectric constant and the lines are fits using the Vogel–Fulcher expression (a); the T_0-dependence on δ (b).

at about 150 K. The dielectric data at low temperatures result in broad loss peaks indicating a wide distribution of relaxation times. The analysis of the complex dielectric permittivity data by means of the Cole–Cole model and the Tikhonov regularization technique demonstrates that the relaxation time distribution becomes strikingly asymmetric at temperatures below 50 K and, consequently, the Cole–Cole analysis is then no longer correct. From the best fit, the temperature dependence of the most probable relaxation time has been extracted. It follows a Vogel–Fulcher law with the Vogel–Fulcher temperature $T_0 = 26$ K. The Kutnjak analysis results in nearly the same temperature, $T_0 = 25$ K. For the protonated sample $BP_{0.15}BPI_{0.85}$, Kutnjak analysis gives $T_0 = 10$ K, whereas because of the low Vogel–Fulcher temperature the most probable relaxation time roughly follows an Arrhenius law [9] within the experimental accuracy. The striking change of the Vogel–Fulcher temperature due to deuteration clearly indicates the importance of quantum tunnelling in $BP_{0.15}BPI_{0.85}$ mixed crystals.

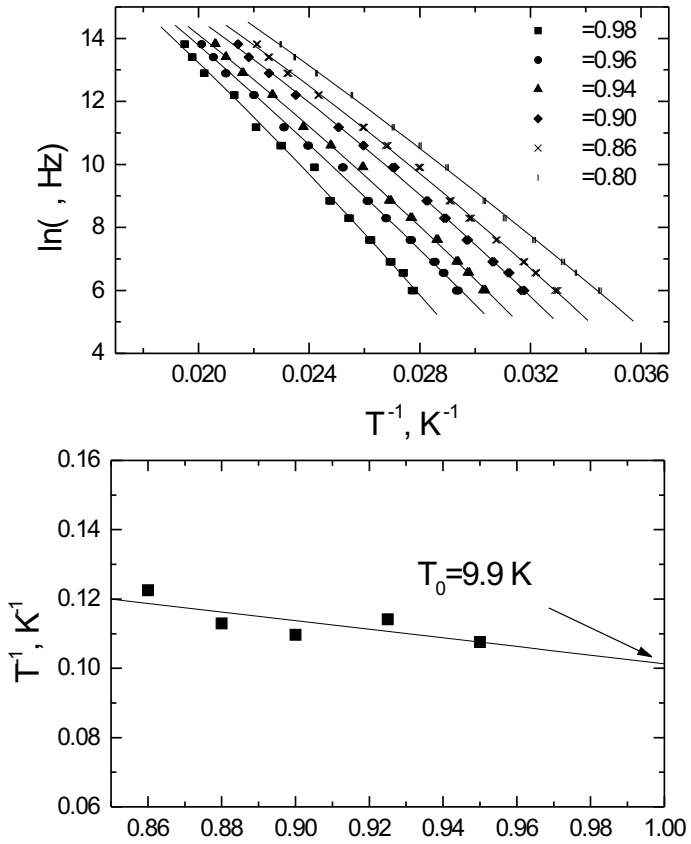

Figure 7. The Arrhenius representation (δ-plot) of $BP_{0.15}BPI_{0.85}$ where the points are obtained from the reduced dielectric constant and the lines are fits using the Vogel–Fulcher expression (a); the T_0-dependence on δ (b).

Acknowledgments

The authors are grateful to Professor Dr R Böttcher and Dr A Pöppl for stimulating and helpful discussions. This work was supported by the 'Alexander von Humboldt Stiftung' and by the 'Deutsche Forschungsgemeinschaft'.

References

[1] Albers J 1988 *Ferroelectrics* **78** 3
Schaack G 1990 *Ferroelectrics* **104** 147
[2] Albers J, Klöpperpieper A, Rother H J and Ehses K 1982 *Phys. Status Solidi* a **74** 553
[3] Schildkamp W and Spilker J Z 1984 *Z. Kristallogr.* **168** 159
[4] Albers J, Klöpperpieper A, Rother H J and Haussühl S 1988 *Ferroelectrics* **81** 27
[5] Santos M L, Azevedo J C, Almeida A, Chaves M R, Pires A R, Müser H E and Klöpperpieper A 1990 *Ferroelectrics* **108** 363
[6] Santos M L, Chaves M R, Almeida A, Klöpperpieper A, Müser H E and Albers J 1993 *Ferroelectr. Lett.* **15** 17
[7] Hutton S L, Fehst I, Böhmer R, Braune M, Mertz B, Lunkenheimer P and Loidl A 1991 *Phys. Rev. Lett.* **66** 1990
[8] Banys J, Sobiestianskas R, Klimm C and Völkel G 1997 *Lithuanian J. Phys.* **37** 505

[9] Banys J, Klimm C, Völkel G, Bauch H and Klöpperpieper A 1994 *Phys. Rev.* B **50** 16 751
[10] Tadic B, Pirc R and Blinc R 1988 *Phys. Rev.* B **37** 679
[11] Bauch H, Banys J, Böttcher R, Pöppl A, Völkel G, Klimm C and Klöpperpieper A 1995 *Ferroelectrics* **163** 59
[12] Banys J, Klimm C, Völkel G, Kajokas A and Klöpperpieper A 1997 *J. Phys.: Condens. Matter* **9** L7
[13] Bauch H, Völkel G, Böttcher R, Pöppl A, Schäfer H, Banys J and Klöpperpieper A 1996 *Phys. Rev.* **54** 9162
[14] Völkel G, Bauch H, Böttcher R, Pöppl A, Schäfer H and Klöpperpieper A 1997 *Phys. Rev.* B **55** 12 151
[15] Schäfer H, Sternin E, Stanarius R, Arndt M and Kremer F 1996 *Phys. Rev. Lett.* **76** 2177
[16] Kutnjak Z, Pirc R, Levstik A, Levstik I, Filipic C, Blinc R and Kind R 1994 *Phys. Rev.* B **50** 12 421
[17] Fischer G, Brückner H J, Klöpperpieper A, Unruh H-G and Levstik A 1990 *Z. Phys.* B **79** 301
[18] Höchli U T 1982 *Phys. Rev. Lett.* **48** 1494
[19] Courtens E 1984 *Phys. Rev. Lett.* **52** 69
[20] Howell F L, Pinto N J and Schmidt V H 1992 *Phys. Rev.* B **46** 13 762
[21] Trybula Z, Schmidt V H and Drumheller J E 1991 *Phys. Rev.* B **43** 1287
[22] Höchli U T, Knorr K and Loidl A 1990 *Adv. Phys.* **39** 405
[23] Hill R M and Jonsher A K 1983 *Contemp. Phys.* **24** 75
[24] Wong J and Angell C A 1976 *Glass: Structure by Spectroscopy* (New York: Dekker)
[25] Binder K and Young A P 1986 *Rev. Mod. Phys.* **58** 801
[26] Cole K S and Cole R H 1941 *J. Chem. Phys.* **19** 1484
[27] Bauch H, Böttcher R and Völkel G 1993 *Phys. Status Solidi* b **179** K41
[28] Sobiestianskas R, Grigas J, Czapla Z and Dacko S 1993 *Phys. Status Solidi* a **136** 223
[29] Fehst I, Böhmer R, Ott W, Loidl A, Bostoen C and Haussühl S 1990 *Phys. Rev. Lett.* **64** 3139
[30] Kim Bog-Gi and Kim Jong-Jean 1998 *Ferroelectrics* **206**79
[31] Dolinsek J, Acron D, Zalar B, Pirc R, Blinc R and Kind R 1996 *Phys. Rev.* B **54** R6811